Luminescent spectroscopy of Pr^{3+} ions in some phosphates, borates and silicates using x-ray synchrotron radiation from VEPP-3 storage ring

Cite as: AIP Conference Proceedings **2299**, 080002 (2020); https://doi.org/10.1063/5.0030875
Published Online: 17 November 2020

Sviatoslav Kiselev, Vladimir Pustovarov, and Marco Bettinelli

Luminescent Spectroscopy of Pr^{3+} Ions in Some Phosphates, Borates and Silicates using X-ray Synchrotron Radiation from VEPP-3 Storage Ring

Sviatoslav Kiselev[1, a)], Vladimir Pustovarov[1, b)] and Marco Bettinelli[2, c)]

[1]*Institute of Physics and Technology, Ural Federal University, 19 Mira st., Ekaterinburg, 620002, Russia*
[2]*Laboratory of Luminescent Materials, Department of Biotechnology, University of Verona and INSTM, UdR Verona, Strada Le Grazie 15, I-37134 Verona, Italy*
[a)]Corresponding author: sviat-kiselev@yandex.ru
[b)]v.a.pustovarov@urfu.ru
[c)]marco.bettinelli@univr.it

Abstract. This paper reports the spectroscopic properties of praseodymium-doped phosphates, borates and silicates. Polycrystalline samples of Pr^{3+}-doped $KLuP_2O_7$, $Li_6Y(BO_3)_3$, $LiY_6O_5(BO_3)_3$, $LiSrPO_4$, $Sr_9Sc(PO_4)_7$, $K_3Lu(PO_4)_2$, $K_3LuSi_2O_7$ were synthesized using a solid state reaction. Spectra of X-ray excited luminescence and its decay kinetics were measured. Studied samples demonstrate interconfigurational 5*d*-4*f*, intraconfigurational 4*f*-4*f* transitions and defect-related luminescence. Comparative analysis of spectroscopic properties and application perspectives is presented.

INTRODUCTION

Inorganic scintillating materials are being actively investigated in terms of their application in fields of nuclear physics, medicine tomography and detecting systems. Industry is highly required in fast time response scintillators. This means that luminescence lifetime has to be as small as possible. Novel researches are devoted to praseodymium-doped compounds. Most existing scintillator systems are based on Ce^{3+} ions. Pr^{3+} ions impurity luminescence has an advantage in higher emission energy and shorter luminescence lifetime (20-30 ns instead of 40-70 in Ce^{3+}) [1]. As well as commercially used scintillators activated with Ce^{3+} ions, Pr^{3+}-doped scintillators are mostly interesting due to the presence of $5d \rightarrow 4f$ electric–dipole emission. The Pr^{3+} $5d \rightarrow 4f$ emission appears, when a sufficiently strong crystal field shifts the lowest $4f^15d^1$ excited state below the $^1S_0$ level [2]. Perfect timing and appropriate emission energy region are such factors that make praseodymium impurity perspective for application potentials in various scintillating systems. It has to be mentioned, that some of studied materials have already been presented in Refs. [3-6].

OBJECTS AND EXPERIMENT DETAILS

Polycrystalline samples of Pr^{3+}-doped $KLuP_2O_7$, $Li_6Y(BO_3)_3$, $LiY_6O_5(BO_3)_3$, $LiSrPO_4$, $Sr_9Sc(PO_4)_7$, $K_3Lu(PO_4)_2$, $K_3LuSi_2O_7$ were synthesized using a solid state reaction and XRD verified for phase purity at the Laboratory of Luminescent Materials, University of Verona (Italy).

$KLuP_2O_7$ (1 mol.% Pr^{3+}): Powder microcrystalline material has a stoichiometry of $KLu_{0.99}Pr_{0.01}P_2O_7$ (*i.e.* containing 1 mol.% Pr^{3+} substituting for Lu^{3+}). The constituent high purity raw materials KNO_3, $(NH_4)_2HPO_4$, Lu_2O_3, and Pr_6O_{11} (the last two reagents 4N) were mixed and heat treated in a horizontal furnace in air for 1 h at 400 ºC and 24 h at 750 ºC with intermediate regrinding. The phase purity of the prepared sample was examined using powder X-ray diffraction (PXRD) technique with a Thermo ARL X'TRA powder diffractometer, operating in the

Synchrotron and Free Electron Laser Radiation
AIP Conf. Proc. 2299, 080002-1–080002-7; https://doi.org/10.1063/5.0030875
Published by AIP Publishing. 978-0-7354-4033-3/$30.00

Bragg-Brentano geometry and equipped with a Cu anode X-ray source (K_α, λ =1.5418 Å) with a Peltier Si(Li) cooled solid-state detector. The obtained PXRD pattern was fully compatible with ICDD Card No. 01-076-7386.

$Li_6Y(BO_3)_3$ (1 mol.% Pr^{3+}): XRD analysis shows that LYBO phase is dominant, but the presence of precursor phases as Y_2O_3 and $Li_6B_4O_9$ could be identified. According to Ref. [7], XRD diffractograms of obtained fully correlates with grown $Li_6Y(BO_3)_3$ single crystals.

$LiSrPO_4$ (1 mol.% Pr3+**):** Stoichiometric amounts of $SrCO_3$ (>98%), Li_2CO_3 (>99.0%), $(NH_4)_2HPO_4$ (>99.0%) and Pr_6O_{11} (99.999%) were mixed, pressed to a pellet and introduced in a covered alumina crucible. The pellet was heated at 1300 °C for 3 h in a horizontal furnace under air at atmospheric pressure. The $LiSrPO_4$ orthophosphate possesses a hexagonal structure with lattice parameters a= 5.0040 Å, c= 24.6320 Å and $P6_5$ space group. The XRD pattern revealed perfect matching with the reference ICDD data that indicates the presence of a single phase structure [4].

$Sr_9Sc(PO_4)_7$ (1 mol.% Pr3+**):** The XRD pattern revealed perfect matching with the reference JPCDS data that indicates the presence of a single phase structure [5].

$K_3Lu(PO_4)_2$ (1 and 5 mol.% Pr3+): K_2CO_3 (99%), $(NH_4)_2HPO_4$ (>99%), Lu_2O_3 (Aldrich, 99,99 %) and Pr_6O_{11} (Aldrich, 99.999%) powders were mixed and pressed into pellets under a load of 10 tons. The samples underwent two thermal treatments under air atmosphere (600 °C for 4 h and 950 °C for 1 h), with intermediate grindings. At room temperature this host crystallizes with a trigonal unit cell, $\overline{P}3$ space group. For this host material two phase transitions are known to occur at lower temperature around 250 and 140 K [8, 9, 10]. All the diffraction peaks in the XRD pattern of 1% Pr^{3+} doped $K_3Lu(PO_4)_2$ sample are compatible with ICDD data of the trigonal $K_3Lu(PO_4)_2$.

$K_3LuSi_2O_7$ (1 mol.% Pr3+): possesses a hexagonal structure, $P6_3$ space group with lattice parameters a = 5.71160(10) Å and c = 13.8883(6) Å [11]. The XRD pattern revealed perfect matching with the reference ICDD data that indicates the presence of a single phase structure [5].

The measurements of decay kinetics and emission spectra upon excitation with non-monochromatic X-ray synchrotron radiation (E = 3–60 keV, pulse FWHM ~ 1 ns, frequency ~ 8 MHz) were performed at the beamline #6 of the VEPP-3 storage ring at Budker Institute of Nuclear Physics (Russia). Stroboscopic method of electron-optical chronography with sub-nanosecond time resolution was used. The detection system included a SOL Instruments MS2004 monochromator equipped with a high-speed LI-602 dissector [12].

For comparison, the pulsed cathodoluminescence (PCL) spectra and PCL decay kinetics were measured using Radan-330A pulse electron gun (E = 120 keV, pulse FWHM = 200 ps, rate 5 Hz) at University of Tartu (Estonia). A 0.3 m Andor Shamrock 303i monochromator equipped with a MCP-PMT detector was used for the registration [13].

RESULTS AND DISCUSSION

Phosphates

Figure 1, (a) presents the results of X-ray excited luminescence spectroscopy of studied phosphates – $KLuP_2O_7$, $K_3Lu(PO_4)_2$, $Sr_9Sc(PO_4)_7$, $LiSrPO_4$. The spectrum of $KLuP_2O_7$ is dominated by emission bands corresponding to $4f^15d^1 \rightarrow 4f^2$ interconfigurational radiative transitions in Pr^{3+} ion. In the region of 380-560 nm (2.21 – 3.26 eV) wide weak bands of defect-related luminescence are observed. Weak emission lines corresponding to intraconfigurational $4f^2 \rightarrow 4f^2$ transitions are located near 490 and 612 nm. The features of XRL spectra indicate the presence of energy transfer from the host to both Pr^{3+} impurity centers and defects. This fact should obviously limit the quantum yield for recombinational luminescence of Pr^{3+} impurity centers due to formation of competing path for capture of charge carriers. According to XRD analysis [8, 10] XRL spectrum of 1% Pr^{3+} $K_3Lu(PO_4)_2$ corresponds to the trigonal phase and XRL spectrum of 5% Pr^{3+} $K_3Lu(PO_4)_2$ corresponds to the monoclinic phase of the investigated crystal. This means that increasing the concentration of Pr^{3+} ions shifts the phase transition from monoclinic to trigonal phases to a temperature higher than 295 K. The yield of $4f^2 \rightarrow 4f^2$ transitions in $Sr_9Sc(PO_4)_7$ is about 9 times more than $4f^15d^1 \rightarrow 4f^2$ output. This occurs because of big Stokes shift. As investigated in [2], the domination of interconfigurational transitions is possible only with Stokes shift smaller than 3200 cm^{-1}. The value of *d-f*/*f-f* ratio is as bigger as the shift is lower. The contribution of defect-related luminescence in $Sr_9Sc(PO_4)_7$ emission spectrum is rather high, what indicates a significant role of this charge carriers capture channel in light output, decreasing the yield of inter- and intraconfigurational transitions. $LiSrPO_4$ emission spectrum contains a set of bands for two transition types – $4f^15d^1 \rightarrow 4f^2$ at 240 and 267 nm and $4f^2 \rightarrow 4f^2$ in 580-650 nm region. *d-f*/*f-f* ratio here is rather high (about 3.25) but potassium compounds are better in this respect – they present 14.28 and 9.1 for $K_3Lu(PO_4)_2$ with 1

% and 5 % praseodymium impurity and 12.5 for $KLuP_2O_7$. The role of this ratio will be discussed later in Comparison chapter.

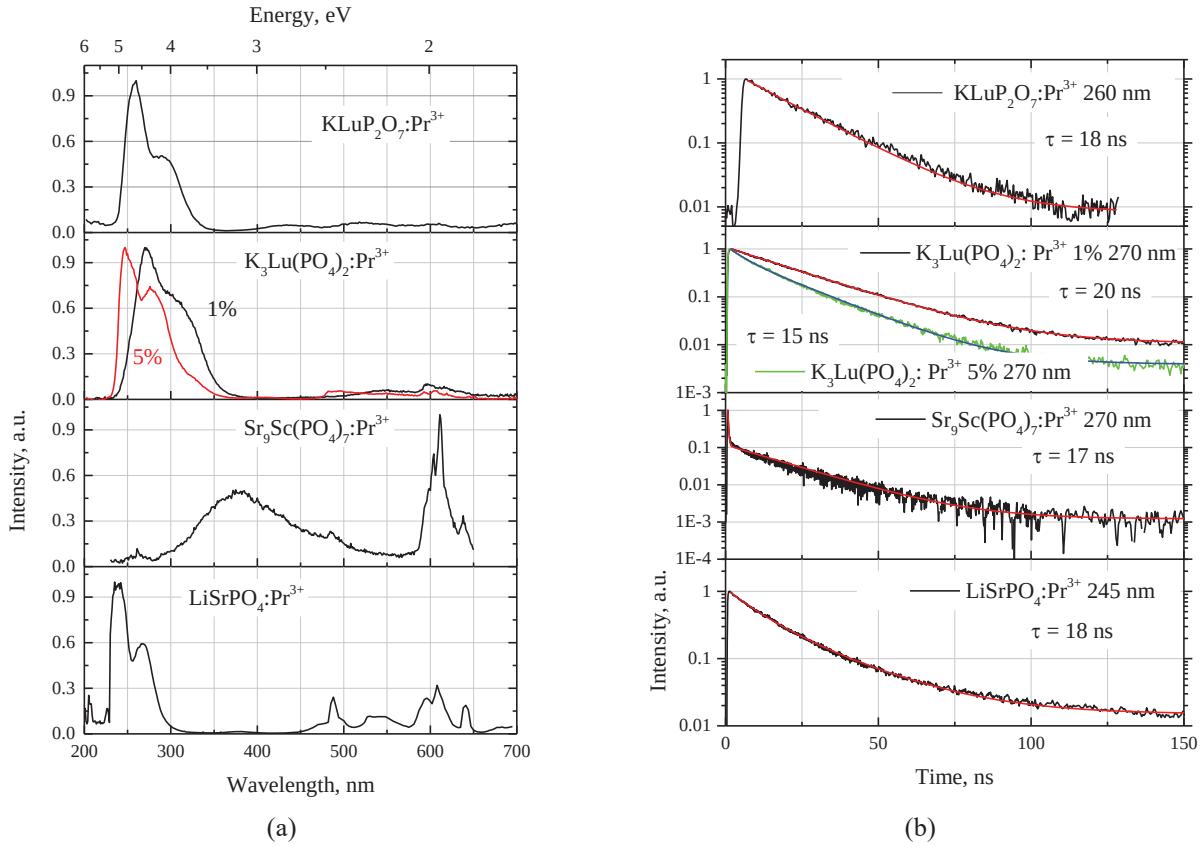

FIGURE 1. (a): XRL spectra of studied phosphates at T = 295 K. (b): Luminescence decay kinetics recorded monitoring main emission bands with λ_{emis} mentioned in the graph excited with high frequency X-ray synchrotron radiation, T = 295 K (black and green curves), approximation lines (red and blue).

For better understanding it must be underlined that luminescence decay kinetics curves in most cases are well fitted with multiexponential approximation (1):

$$I(t)=I_0+\sum A_i \cdot \exp\left(-\frac{t}{\tau_i}\right) \quad (1)$$

Here, I_0 is the contribution of background level describing the role of slow components. A_i has to amount the amplitude maximum of each exponential component with τ_i as lifetime.

Figure 1, (b) is devoted to luminescence decay kinetics of $d \rightarrow f$ emission bands of samples presented in Fig. 1, (a). The XRL decay curve of $KLuP_2O_7$ demonstrates nearly single exponential decay behavior without any noticeable build-up stage with lifetime of 18.4 ns. The $d \rightarrow f$ emission decay kinetics of $K_3Lu(PO_4)_2$ is well fitted the two-exponential approximation with parameters: τ_1~5 ns and τ_2~20.5 ns. $Sr_9Sc(PO_4)_7$ reveals a fast component (τ~15 ns) while the contribution of the slow µs decay component reaches 18%. Decay kinetics of $LiSrPO_4$ is very same as in $KLuP_2O_7$, and it is described with same lifetime of 18 ns. From presented kinetics the only material with noticeable build-up stage is $Sr_9Sc(PO_4)_7$. We suppose that presence of this stage is caused with defect-related luminescence and energy transfer from impurity ions to host defects.

Borates

X-ray excited luminescence emission spectra of $Li_6Y(BO_3)_3$ and $LiY_6O_5(BO_3)_3$ are presented in Fig. 2, (a). Wide bands in UV region (270-310 nm) with nanosecond decay time excited with synchrotron radiation pulse are

connected with interconfigurational $4f^15d \rightarrow 4f^2$ radiation transitions with different Stokes shift (Fig. 2, (a)). These transitions are considered to be the emission from the lowest $4f^15d$ excited state of the Pr^{3+} ion to the multiplets of ground states of the $4f^2$ configuration.

Narrow lines in visible region correspond to intraconfigurational $4f^2 \rightarrow 4f^2$ transitions in Pr^{3+} ions. The identification of $4f^2 \rightarrow 4f^2$ transitions is based on Dike's diagram [2]. Those lines show $^3P_2 - {}^3F_2$ (605 nm) and $^1D_2 - {}^3H_6$ (665 nm) radiation transitions. XRL spectrum makes possible to detect and recognize them. A set of wide emission bands in region of ~ 400-500 nm considered to be defect-related. Previously made measurements of photoluminescence excitation spectra in [6] make it possible to declare that an efficient transport of energy from the impurity center to the defect exists. This limits the recombination luminescence output of the Pr^{3+} impurity center, creating a competing charge carrier capture channel.

$LiY_6O_5(BO_3)_3$ XRL emission spectrum is very different from phosphates spectra discussed above. Here, we observe only tends of intraconfigurational $4f^2 \rightarrow 4f^2$ transitions in 580-650 nm region. So, *d-f*/*f-f* ratio is the lowest one from all examined objects. This fact allows us to clarify that potential of $LiY_6O_5(BO_3)_3$ in terms of searching of inorganic scintillating material with fast interconfigurational $5d$-$4f$ transitions is unacceptable for making any comparison with other powders.

XRL decay kinetics of $Li_6Y(BO_3)_3$ (Fig. 2, (b)) was also fitted with two-exponential approximation. The decay time of 275 nm emission band amounts 16.7 ns for fast component and ~ 49 ns for second ns-component. 400 nm emission peak's decay kinetics has other characteristics: 11.1 ns for first fast component and ~ 80 ns for second ns-component. Slow μs-component influence is rather high; its order is 10^{-2}.

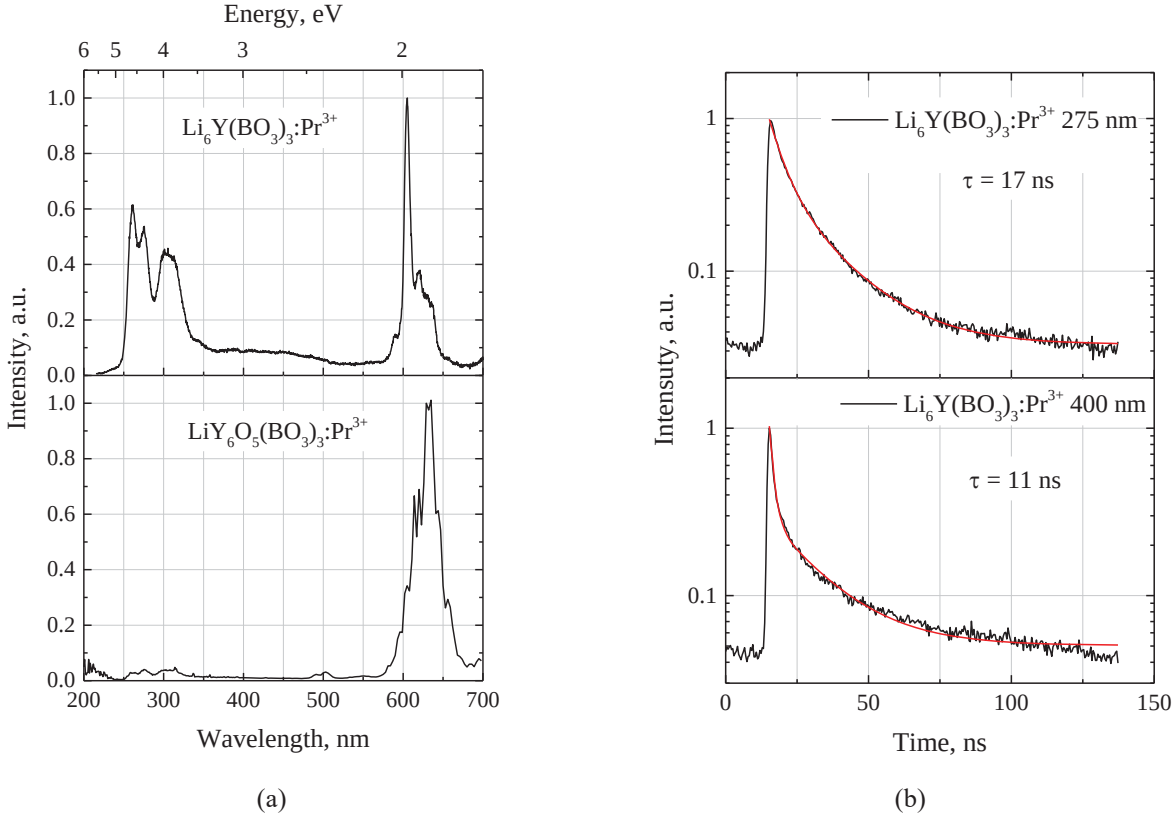

FIGURE 2. (a): XRL spectra of studied borates at T = 295 K. (b): Luminescence decay kinetics recorded monitoring main emission bands with λ_{emis} mentioned in the graph excited with high frequency X-ray synchrotron radiation, T = 295 K (black curves), approximation lines (red).

To analyze the behaviour of decay kinetics curves, Fig. 3 contains the data of pulse cathode luminescence (PCL) kinetics (a) and luminescence kinetics excited with high frequency (8 MHz) X-ray synchrotron radiation (b). Both lines for $4f^15d \rightarrow 4f^2$ emission and defect-related luminescence (region of 350 – 500 nm) are presented.

The PCL decay curves demonstrate two-exponential decay behaviour without any noticeable build-up stage. Decay curves are dominated by a main fast component with lifetime of 10.1 ns. The more slow decay component has a lifetime of about 70 ns. The contribution of slow μs – component is $10^{-3} - 10^{-4}$. XRL decay kinetics was also

fitted with two-exponential approximation. The decay time of 275 nm emission band amounts 16.7 ns for fast component and ~ 49 ns for second ns- component. 400 nm emission peak's decay kinetics has other characteristics: 11.1 ns for first fast component and ~ 80 ns for second ns-component. Slow μs-component influences more than in PCL decay kinetics; its order is 10^{-2}. Both X-ray and cathode ray excited decay kinetics of interconfigurational transitions show no build-up stage. Their close values demonstrate that electron-hole recombination in Pr^{3+} ion does not delay the immediate population of Pr^{3+} $4f^15d^1$ excited state. The build-up stage in defect-related luminescence kinetics may indicate the presence of shallow traps which act as intermediate trapping centers for thermalized charge carriers; this can be approved in thermally stimulated luminescence measurements.

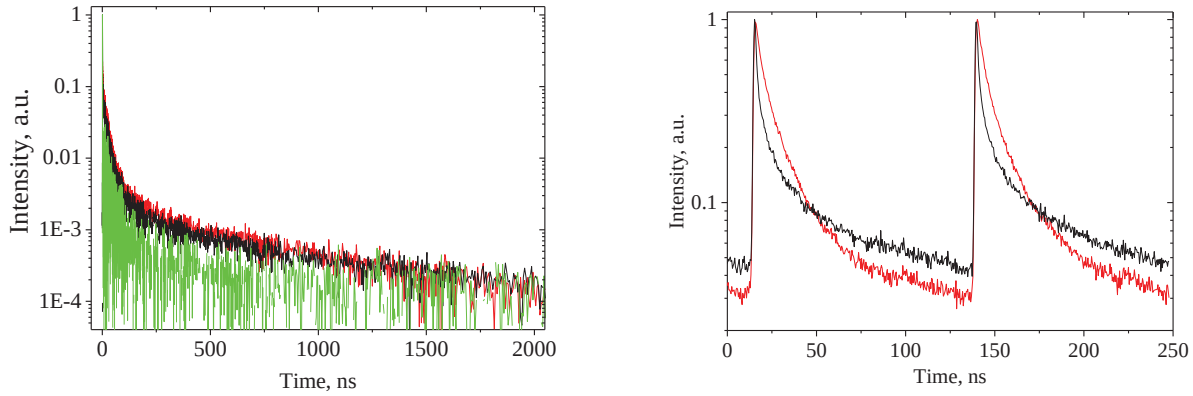

(a) (b)

FIGURE 3. (a): PCL decay kinetics recorded monitoring $4f^15d \rightarrow 4f^2$ emission in $Li_6Y(BO_3)_3:Pr^{3+}$ at 260 (black), 275 (red) and 400 nm (green). (b): XRL decay kinetics recorded monitoring $4f^15d \rightarrow 4f^2$ emission of $Li_6Y(BO_3)_3:Pr^{3+}$ at 275 (red) and 400 nm (black) excited with high frequencies X-ray synchrotron radiation. T= 295 K

Silicates

The XRL yield of $K_3LuSi_2O_7$ (Fig. 4, (a)) demonstrates no sign of defect-related luminescence, only typical bands of $d \rightarrow f$ and $f \rightarrow f$ transitions are presented. Light yield of both types are almost identical due to big Stokes shift. The $d \rightarrow f$ emission decay kinetics of $K_3LuSi_2O_7$ (Fig. 4, (b)) departs from an exponential behavior and demonstrates the presence of intense slow decay component appearing as a background. Luminescence lifetime of main component in decay kinetics is 54 ns, which is too slow in comparison with phosphates compounds. The presence of the build-up stage in the decay kinetics of $K_3LuSi_2O_7$ indicates intermediate localization of charge carriers at the capture centers before their recombination at the impurity center.

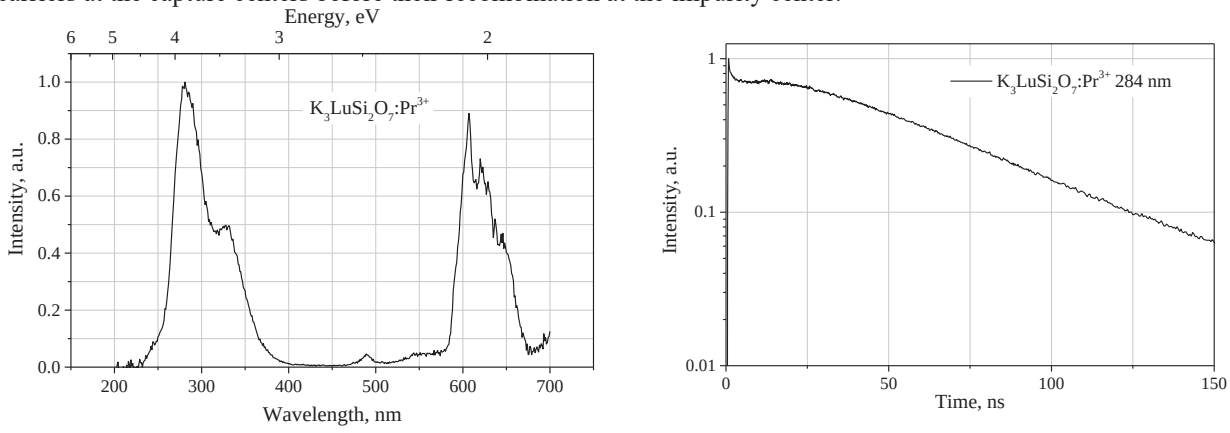

(a) (b)

FIGURE 4. (a): XRL spectra of studied silicates at T = 295 K. (b): Luminescence decay kinetics recorded monitoring main emission bands with λ_{emis} mentioned in the graph excited with high frequency X-ray synchrotron radiation, T = 295 K.

Comparison

Results discussion is summarized in Table 1. Here, we want to demonstrate the main peculiarities of studied samples. Wavelength region of interconfigurational transitions is from 240 to 327 nm (3.79 – 5.16 eV) for all compounds. Emission lifetime varies from 15 to 54 ns. The best timing belongs to $K_3Lu(PO_4)_2:Pr^{3+}$ (5 %). The last column present calculated ratio of interconfigurational to intraconfigurational transitions – $K_3Lu(PO_4)_2:Pr^{3+}$ (5 %) also has the best ratio in this respect. Also, it has to be underlined that such materials as $K_3Lu(PO_4)_2$: Pr^{3+} (1 %), $KLuP_2O_7$: Pr^{3+} (1 %) and $LiSrPO_4$: Pr^{3+} (1 %) possess a good set of characteristics satisfying to investigated properties in terms of new scintillating materials.

TABLE 1. Comparative characteristics of polycrystalline samples doped with Pr^{3+} ion, T= 295 K

Material	Z_{eff}	λ_{max}, nm	τ, ns	d-f/f-f
$Sr_9Sc(PO_4)_7$: Pr^{3+} (1 %)	27.0	261; 300	17	0.12
$LiSrPO_4$: Pr^{3+} (1 %)	36.8	240; 267	18	3.25
$K_3Lu(PO_4)_2$: Pr^{3+} (1 %)	37.6	270; 308	20	9.10
$K_3Lu(PO_4)_2$: Pr^{3+} (5 %)	37.6	246; 278	15	14.28
$KLuP_2O_7$: Pr^{3+} (1 %)	41.6	258; 292	18	12.51
$Li_6Y(BO_3)_3$: Pr^{3+} (1%)	20.0	261; 305	17	0.62
$LiY_6O_5(BO_3)_3$: Pr^{3+} (1%)	32.1	274; 309	-	0.05
$K_3LuSi_2O_7$: Pr^{3+} (1%)	64.9	279; 327	54	1.14

The relative ratio of *d→f/f→f* transitions yield depends on excitation energy and measurement temperature. At room temperature *d→f/f→f* ratio is lower with band to band excitation than at inner-center excitation. According to Srivastava et al. [4], in order to produce the domination of $4f^15d \rightarrow 4f^2$ emission over intraconfigurational $4f^2 \rightarrow 4f^2$ transitions, the compound has to demonstrate small Stokes shift. In Pr^{3+} ion this threshold amounts 3200 cm^{-1}, or 0.4 eV. If both types of emission lines can be observed in studied sample, it can be concluded then, that the reason of their presence is big Stokes shift.

CONCLUSION

The spectroscopic properties of praseodymium-doped phosphates, borates and silicates are studied in this report. Polycrystalline samples of Pr^{3+}doped $KLuP_2O_7$, $Li_6Y(BO_3)_3$, $LiY_6O_5(BO_3)_3$, $LiSrPO_4$, $Sr_9Sc(PO_4)_7$, $K_3Lu(PO_4)_2$, $K_3LuSi_2O_7$ were synthesized using a solid state reaction. Spectra of X-ray excited luminescence and its kinetics were measured at the beamline #6 of the VEPP-3 storage ring at Budker Institute of Nuclear Physics (Novosibirsk). Studied samples demonstrate interconfigurational 5*d*-4*f*, intraconfigurational 4*f*-4*f* transitions and defect-related luminescence. Comparative analysis of spectroscopic properties and application perspectives is presented. Based on luminescence lifetime, *d-f/f-f* ratio and emission energy region parameters the conclusion of most perspective material for application in scintillator systems is made. In our opinion, these materials are $K_3Lu(PO_4)_2:Pr^{3+}$ (5 %), $K_3Lu(PO_4)_2$: Pr^{3+} (1 %), $KLuP_2O_7$: Pr^{3+} (1 %) and $LiSrPO_4$: Pr^{3+} (1 %). Their order is from most perspective to the worst one. Naturally, to produce the entire conclusion of material application potential a thorough analysis is needed implying studying other types of excitation and temperature research.

ACKNOWLEDGMENT

The work was partially supported by the Ministry of Science and Higher Education of the Russian Federation (through the basic part of the government mandate, project No. FEUZ-2020-0060), Act 211 Government of the Russian Federation (contract № 02.A03.21.0006) and RFMEFI62117X0012 project. The time-resolved X-ray excited measurements were performed at the Shared research center SSTRC based on the NovoFEL/VEPP-4 -

VEPP-2000 facilities at Budker Institute of Nuclear Physics (Siberian Branch of Russian Academy of Sciences, Novosibirsk, Russia) while using experimental equipment funded by RFMEFI62119X0022 project. The authors are grateful to S. Omelkov (University of Tartu, Estonia) for assisting in the measurement using a pulsed electron beam.

REFERENCES

1. K.V. Ivanovskikh, Q. Shi, M. Bettinelli, and V.A. Pustovarov, Optical Materials **79**, 108-114 (2018).
2. A.M. Srivastava, J. Luminescence **169**, 445–449 (2016).
3. V.A. Pustovarov, J. Surf. Investigation: X-ray, Synchr. Neutr. Tech. **9**, 1168-1171 (2015).
4. V.A. Pustovarov, K.V. Ivanovskikh, Yu.E. Khatchenko, Q. Shi, and M. Bettinelli, Radiation Measurements **123**, 39-43 (2019).
5. V.A. Pustovarov, K.V. Ivanovskikha, Yu.E. Khatchenko, V.Yu. Ivanov, M. Bettinelli, and Q. Shi, Physics of the Solid State, Vol. **61**, No. 5, 758–762 (2019).
6. S.A. Kiselev and V.A. Pustovarov, AIP Conference Proceedings **2174**, 020120 (2019).
7. É. Tichy-Rács, Á. Péter, V. Horváth, K. Polgár, K. Lengyel and L. Kovács, "Preparation and study of $Li_6Y(BO_3)_3$ and $Li_6Gd(BO_3)_3$ double borates," in *Materials Science Forum-729*, Trans. Tech. Publications, Edited by T. Berecz (Trans Tech Publication, Switzerland, 2013), pp. 493–496.
8. M. Trevisani, K.V. Ivanovskikh, F. Piccinelli, M. Bettinelli, J. Lumin. **152**, 2-6 (2014).
9. D. Wisniewski, A.J. Wojtowicz, W. Drozdowski, J.M. Farmer, L.A. Boatner, J. of Alloys and Compounds **380**, 191-195 (2004).
10. I. Carrasco, K. Bartosiewicz, F. Piccinelli, M. Nikl, M. Bettinelli, J. of Lumin. **189**, 113–119 (2017).
11. I. Vidican, M.D. Smith, H.-C. zur Loye, J. Solid State Chem. **170**, 203-210 (2003).
12. V.A. Pustovarov, E.I. Zinin, A.L. Krymov, B.V. Shulgin, Rev. Sci. Instrum. **63**, 3521 (1992).
13. S.I. Omelkov, V. Nagirnyi, E. Feldbach, R. M. Turtos, E. Auffray, M. Kirm, P. Lecoq, J. Lumin. **191** A, 61-67 (2017).
14. A.M. Srivastava, M. Jennings, J. Collins, Opt. Mater. **34**, 1347 (2012).